Available online at www.sciencedirect.com
SCIENCE DIRECT®
ELSEVIER
International Journal of Solids and Structures 43 (2006) 1388–1403
INTERNATIONAL JOURNAL OF SOLIDS and STRUCTURES
www.elsevier.com/locate/ijsolstr

A semi-analytical solution for static and dynamic analysis of plates with piezoelectric patches

Guanghui Qing [a,*], Jiajun Qiu [b], Yanhong Liu [a]

[a] *Aeronautical Mechanics and Avionics Engineering College, Civil Aviation University of China, Tianjin 300300, People's Republic of China*
[b] *Department of Mechanics and Engineering Measurement, School of Mechanical Engineering, Tianjin University, 92, Weijin Road, Tianjin 300072, People's Republic of China*

Received 27 August 2004
Available online 21 April 2005

Abstract

A modified mixed variational principle for piezoelectric materials is established and the state-vector equation of piezoelectric plates is deduced directly from the principle. Then the exact solution of the state-vector equation is simply given, and based on the semi-analytical solution of the state-vector equation, a realistic mathematical model is proposed for static analysis of a hybrid laminate and dynamic analysis of a clamped aluminum plate with piezoelectric patches. Both the plate and patches are considered as two three-dimensional piezoelectric bodies, but the same linear quadrilateral element is used to discretize the plate and patches. This method accounts for the compatibility of generalized displacements and generalized stresses on the interface between the plate and patches, and the transverse shear deformation and the rotary inertia of the plate and patches are also considered in the global algebraic equation system. Meanwhile, there is no restriction on the thickness of plate and patches. The model can be also modified to achieve a semi-analytical solution for the transient responses to dynamic loadings and the vibration control of laminated plate with piezoelectric patches or piezoelectric stiffeners.

Keywords: Modified mixed variational principle; State-vector equation; Semi-analytical solution; Laminated plates; Piezoelectric patches

* Corresponding author. Tel.: +86 222 409 3144; fax: +86 222 409 2400.
E-mail address: qingluke@126.com (G. Qing).

0020-7683/$ - see front matter © 2005 Elsevier Ltd. All rights reserved.
doi:10.1016/j.ijsolstr.2005.03.048

1. Introduction

Due to their wide application, the laminated piezoelectric plate, hybrid laminates, or the conventional plate with piezoelectric sensor and actuator patches, as shown in Fig. 1, have stimulated considerable studies on the electric and mechanical behaviors of piezoelectric structures. For the piezoelectric laminates or hybrid laminate, one of the main methods conducted is the exact solution. Because of their analytical nature, the exact solutions of static and vibrations analysis of the laminates are of particular value. These solutions can predict exactly the static deformation, generalized stresses, the natural frequencies of the system and the corresponding mode shapes, particularly, as the physical quantities are near or across the interface of dissimilar material layers, and can thus be used to check the accuracy of various numerical methods for more complicated problems (Pan and Heyliger, 2002). Meanwhile, the exact solutions can provide the distributions figures of generalized displacements and stresses. Most of the published works on the exact solutions for laminated composite, the laminated piezoelectric beams/plates or the hybrid laminates can be divided into two groups. The methods used in the first group (Ray et al., 1993a,b; Ray et al., 1998; Batra

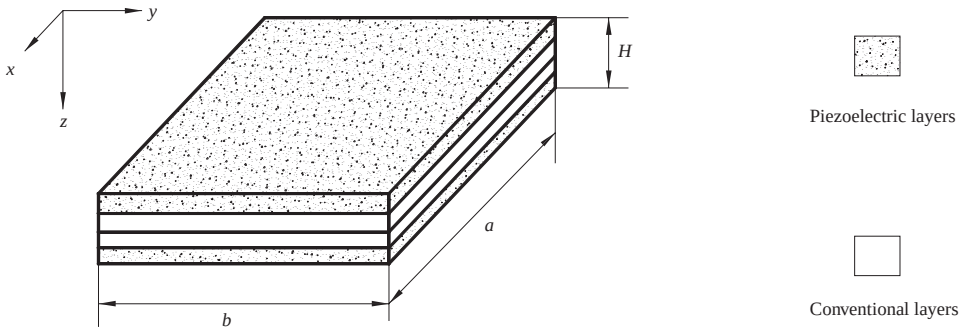

(a) A hybrid laminate

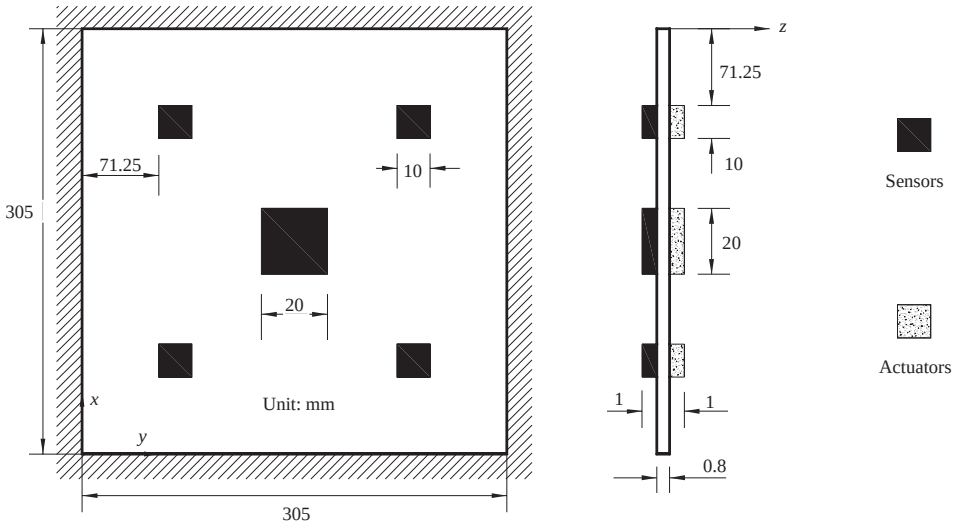

(b) Clamped smart plate with piezoelectric sensors/actuators

Fig. 1. Geometry of piezoelectric plates: (a) a hybrid laminate and (b) clamped smart plate with piezoelectric sensors/actuators.

and Liang, 1997; Senthil and Batra, 2001; Heyliger, 1994, 1997; Heyliger and Saravanos, 1995; Heyliger and Brooks, 1995, 1996) mostly follow the strategies of Pagano (1969, 1970, 1972). The second group (Lee and Jiang, 1996; Aldraihem and Khdeir, 2003a,b; Vel and Batra, 2000; Pan, 2001; Pan and Heyliger, 2002; Ding and Tang, 1999; Tarn, 2002; Wang et al., 2002, 2003; Chen et al., 2004) follows the strategies of Eshelby–Stroh formulation or state-vector equation. The common feature of the strategies of the Eshelby–Stroh formulation and the state-vector equation is that the generalized displacements and stresses are treated simultaneously as the components of the multi-dimensional vector. Hence, the strategies can be called mixed state variable techniques. One of advantages using the mixed state variable techniques to handle composite laminates and piezoelectric laminates is the varying material and geometric properties along the independent spatial variable are allowed, and anisotropic layered materials can be handled (Steele and Kim, 1992; Ting, 1996). Another outstanding advantage is that the thick plates or laminated plates problems can be treated without any displacements and stresses assumptions. Because of the transfer matrix being employed, the order of the final algebra equation system is independent of the thickness and the number of layers of a structure and the solution also provides a continuous transverse stresses field across the thickness of multi-layered structures.

However, owing to the complexity of the governing equations in piezoelectricity, only a few simple problems such as simply supported beams and plates can be solved analytically. Just as Vel and Batra (2000) pointed out, most the available references three-dimensional solutions mentioned above are restricted to the piezoelectric laminates or the hybrid laminates whose edges are simply supported and electrically grounded. Owing to the boundaries and geometric complexity of the practical system in engineering field, it is inevitable that the finite element method (FEM) is required in the design and analysis of piezoelectric structures. The finite element methods for piezoelectric bodies or its devices and adaptive structures can handle numerically a bulk of problems in engineering field and has proved to be a powerful tool for the design and analysis of piezoelectric devices.

A brief review on the finite element models of a structure with sensors and actuators can be found in Kim et al. (1997). Benjeddou (2000) had surveyed the advances and discussed the trends in the formulations and the applications of the finite element modeling of adaptive structural elements.

Because most of the finite element methods for piezoelectric problems are developed from traditional finite element methods, the existence of several issues similar to traditional finite element methods should be noticed: on the one hand, the brick element to model devices as well as large structure regions results in computational models that are artificially large and stiff. On the other hand, the brick element is too thick to modelize very thin structures (Benjeddou, 2000). This motivates the development of one- and two-dimensional elements for the design and analysis of piezoelectric devices. But most of them are free of electric Dofs, standard finite elements are then used to compute mechanical behavior (displacement, strains, stresses), and electric quantities (charge, current, potential) are deduced from the specific sensing/actuation relations.

In a word, there are many challenges in the numerically simulating the behavior of piezoelectric structures and devices where accuracy as well as efficiency of modeling is essential. For instance, traditional finite element methods cannot provide a continuous transverse stresses field across the thickness of a multi-layered structure. The brick elements lead to unnatural stiffening of the plate and artificially high natural frequencies and so on. On the other hand, at present, there are limited modules available for simulating the behavior of piezoelectric structures and devices.

It is worthwhile to notice that the semi-analytical techniques are applied to handle the problems of general composite laminates. The semi-analytical solution (Zou and Tang, 1995; Sheng and Ye, 2002) combines the traditional finite element approximation (using linear quadrilateral element) with the recursive formulation of the state-vector equation. The semi-analytical solution (Zou and Tang, 1995; Sheng and Ye, 2002) inherits most of advantages in the exact solution of state-vector equation. For example, the three-dimensional problem is transferred into the two-dimensional one. The number of variables of the final algebra equation system is independent of the thickness and the number of layers of multi-layered structures;

hence the number of variables is reduced greatly. On the other hand, the semi-analytical solution can also provide continuous transverse stresses across all material interfaces.

It is significant to pursue and develop a semi-analytical solution combining the analytical and FEM techniques for the complicated piezoelectric problems in engineering field.

It should be mentioned that Kim et al. (1997) proposed a novel model that 20-node brick elements are used to model the piezoelectric device regions and nine-node flat-shell elements are used in the remaining part of the plate and transient elements connect brick elements to flat-shell elements. The method has merits in terms of accuracy and economy and was employed in the various vibration controls of piezoelectric structures (Kim et al., 1996, 1997; Lim et al., 2002; Lim, 2003).

In the present work, on the basis of the modified mixed variation principle (Steele and Kim, 1992) for elastic bodies, a similar modified mixed variational principle for piezoelectric material is established. The state-vector equation of piezoelectric plates is derived directly through the use of the present variational formulation. The explicit forms of the generalized displacements and stresses with respect to boundary conditions are given. Then, the exact solution of the state-vector equation is simply given, and the semi-analytical solution of the state-vector equation is achieved. Numerical studies for the static behavior of piezoelectric laminates and the free vibration of a conventional plate with piezoelectric patches are investigated and compared with known results.

2. The formulations

2.1. The modified mixed H-R variational principle

The laminated plate with piezoelectric layer is shown in Fig. 1(a). The piezoelectric layers can be bonded to the surface as well as embedded in the laminates. Assuming the material of each layer is orthotropic and the orthotropic symmetry with respect to the coordinate planes, the linear constitutive equations are written as the following matrix form:

$$\begin{Bmatrix} \sigma_x \\ \sigma_y \\ \sigma_z \\ \tau_{yz} \\ \tau_{xz} \\ \tau_{xy} \\ D_x \\ D_y \\ D_z \end{Bmatrix} = \begin{bmatrix} C'_{11} & C'_{12} & C'_{13} & 0 & 0 & 0 & 0 & 0 & e'_{31} \\ C'_{12} & C'_{22} & C'_{23} & 0 & 0 & 0 & 0 & 0 & e'_{32} \\ C'_{13} & C'_{23} & C'_{33} & 0 & 0 & 0 & 0 & 0 & e'_{33} \\ 0 & 0 & 0 & C'_{44} & 0 & 0 & 0 & e'_{24} & 0 \\ 0 & 0 & 0 & 0 & C'_{55} & 0 & e'_{15} & 0 & 0 \\ 0 & 0 & 0 & 0 & 0 & C'_{66} & 0 & 0 & 0 \\ 0 & 0 & 0 & 0 & e'_{15} & 0 & -\varepsilon'_{11} & 0 & 0 \\ 0 & 0 & 0 & e'_{24} & 0 & 0 & 0 & -\varepsilon'_{22} & 0 \\ e'_{31} & e'_{32} & e'_{33} & 0 & 0 & 0 & 0 & 0 & -\varepsilon'_{33} \end{bmatrix} \begin{Bmatrix} s_x \\ s_y \\ s_z \\ s_{yz} \\ s_{xz} \\ s_{xy} \\ -E_x \\ -E_y \\ -E_z \end{Bmatrix} \tag{1}$$

where, σ_x, σ_y, σ_z, τ_{yz}, τ_{xz} and τ_{xy} are the components of the stress respectively. C'_{ij} $(i,j=1,2,3,4,5,6)$ are elastic coefficients. E_x, E_y, E_z are the components of the electric field. D_x, D_y, D_z are the electric displacements; ε'_{31}, e'_{32}, e'_{33}, e'_{24}, e'_{15} and ε'_{11}, ε'_{22}, ε'_{33} are the piezoelectric, dielectric coefficients, respectively.

The relationships of the mechanical displacement–strain

$$\begin{aligned} &s_x = \alpha u, s_y = \beta v, s_z = \gamma w, s_{yz} = \beta w + \gamma v \\ &s_{xz} = \alpha w + \gamma u, s_{xy} = \beta u + \alpha v \end{aligned} \tag{2}$$

in which u, v and w are the components of displacements and $\alpha = \partial/\partial x$, $\beta = \partial/\partial y$ and $\gamma = \partial/\partial z$ are differential operators.

The electric field components can be related to the electric potential ϕ

$$E_x = -\alpha\phi \quad E_y = -\beta\phi \quad E_z = -\gamma\phi \tag{3}$$

Based on the method that Steele and Kim (1992) and Zhong (1995) established the modified mixed variational principle for elastic bodies, the modified mixed variational principle for three-dimensional piezoelectric plates can be stated as

$$\begin{aligned}\delta\Pi = {} & \delta\int_0^h \left\{\int\int_\Omega L_{MR}\,\mathrm{d}\Omega\right\}\mathrm{d}z - \delta\int_0^h \left\{\int_{\Gamma_u} \mathbf{T}^{\mathrm{T}}(\mathbf{Q}-\overline{\mathbf{Q}})\,\mathrm{d}\Gamma\right\}\mathrm{d}z - \delta\int_0^h \left\{\int_{\Gamma\sigma} \mathbf{Q}^{\mathrm{T}}\overline{\mathbf{T}}\,\mathrm{d}\Gamma\right\}\mathrm{d}z \\ & - \delta\int\int_{\Omega_{\mathrm{t}}} \mathbf{Q}^{\mathrm{T}}\overline{\mathbf{T}}\,\mathrm{d}\Omega - \delta\int\int_{\Omega_{\mathrm{b}}} \mathbf{Q}^{\mathrm{T}}\overline{\mathbf{T}}\,\mathrm{d}\Omega = 0\end{aligned} \tag{4}$$

where

h	is the plate thickness
Ω	is the area of plate
Γ_u	is the generalized displacement boundary
Γ_σ	is the generalized force boundary
Ω_{t}	is the top surface area of plate
Ω_{b}	is the bottom surface area of plate

The superscript 'T' denotes transposition.

The mechanical displacement and electric potential vector

$$\mathbf{Q} = [\,u \quad v \quad w \quad \phi\,]^{\mathrm{T}} \quad \overline{\mathbf{Q}} = [\,\bar{u} \quad \bar{v} \quad \bar{w} \quad \bar{\phi}\,]^{\mathrm{T}}$$

The mechanical stresses and electric displacement vector

$$\mathbf{T} = [\,T_x \quad T_y \quad T_z \quad T_q\,]^{\mathrm{T}} \quad \overline{\mathbf{T}} = [\,\overline{T}_x \quad \overline{T}_y \quad \overline{T}_z \quad \overline{T}_q\,]^{\mathrm{T}}$$

$$L_{MR} = \mathbf{P}^{\mathrm{T}}\dot{\mathbf{Q}} + \mathbf{P}^{\mathrm{T}}(\mathbf{G}_1\mathbf{Q} + \mathbf{\Phi}_{21}^{\mathrm{T}}\mathbf{G}_2\mathbf{Q}) + \frac{1}{2}((\mathbf{G}_2\mathbf{Q})^{\mathrm{T}}\mathbf{\Phi}_{22}\mathbf{G}_2\mathbf{Q} - \mathbf{Q}^{\mathrm{T}}\mathbf{\Omega}\mathbf{Q}) - \frac{1}{2}\mathbf{P}^{\mathrm{T}}\mathbf{\Phi}_{11}\mathbf{P} - \mathbf{Q}^{\mathrm{T}}\mathbf{F} \tag{5}$$

where

$\mathbf{P} = [\,\tau_{xz} \quad \tau_{yz} \quad \sigma_z \quad D_z\,]^{\mathrm{T}}$;
$\mathbf{F} = [\,f_x \quad f_y \quad f_z \quad f_q\,]^{\mathrm{T}}$ denotes the generalized external load;
$\dot{\mathbf{Q}} = \mathrm{d}\mathbf{Q}/\mathrm{d}z$.

The matrices $\mathbf{G}_1$, $\mathbf{G}_2$, $\mathbf{\Phi}_{11}$, $\mathbf{\Phi}_{12}$, $\mathbf{\Phi}_{21}$ and $\mathbf{\Phi}_{22}$ are given in Appendix A.

2.2. The state-vector equation and its exact solution

In the following, assuming the side generalized stress boundaries are satisfied ($\mathbf{T} = \overline{\mathbf{T}}$), and the side generalized displacement boundaries are satisfied ($\mathbf{Q} = \overline{\mathbf{Q}}$). The variational manipulation ($\delta\Pi = 0$) of Eq. (4) is performed without any deformation expression assumption.

Considering the variations of the $\tau_{xz}, \tau_{yz}, \sigma_z, D_z, u, v, w$ and ϕ, respectively, we obtain

$$\begin{aligned}&\frac{\mathrm{d}\mathbf{Q}}{\mathrm{d}z} + (\mathbf{G}_1 + \mathbf{\Phi}_{21}^{\mathrm{T}}\mathbf{G}_2)\mathbf{Q} - \mathbf{\Phi}_{11}\mathbf{P} = 0 \\ &-\frac{\mathrm{d}\mathbf{P}}{\mathrm{d}z} + (\mathbf{G}_1^{\mathrm{T}} + \mathbf{G}_2^{\mathrm{T}}\mathbf{\Phi}_{21})\mathbf{P} + (\mathbf{G}_2^{\mathrm{T}}\mathbf{\Phi}_{22}\mathbf{G}_2 - \mathbf{\Omega})\mathbf{Q} - \mathbf{F} = 0\end{aligned} \tag{6}$$

The mechanical stresses and electric displacement of at the top surface and bottom surface

$$\mathbf{T} = \overline{\mathbf{T}} = \left[n_z\bar{\tau}_{xz} \quad n_z\bar{\tau}_{yz} \quad n_z\bar{\sigma}_z \quad n_{qz}\overline{D}_z \right]^{\mathrm{T}} \tag{7a}$$

in which

The mechanical stresses, electric displacement on the side boundary

$$\begin{aligned}
\overline{T}_x &= n_x(k_{12}\alpha u + k_{13}\beta v - k_8\sigma_z - k_{10}D_z) + n_y k_{15}(\beta u + \alpha v) + n_z\tau_{xz} \\
\overline{T}_y &= n_x k_{15}(\beta u + \alpha v) + n_y(k_{13}\alpha u + k_{14}\beta v - k_9\sigma_z - k_{11}D_z) + n_z\tau_{yz} \\
\overline{T}_z &= n_x\tau_{xz} + n_y\tau_{yz} + n_z\sigma_z \\
\overline{T}_q &= n_{qx}(k_{16}\alpha\phi - k_6\tau_{xz}) + n_{qy}(k_{17}\alpha\phi - k_7\tau_{yz}) + n_{qz}D_z
\end{aligned} \tag{7b}$$

where n_i $(i = x, y, z)$ are the unit outward normal components related to mechanical quantities of the boundary and n_{qi} $(i = x, y, z)$ are the unit outward normal components related to electric quantities of the boundary.

Eq. (6) can be recast into the state-vector form

$$\frac{\mathrm{d}}{\mathrm{d}z}\begin{Bmatrix}\mathbf{P}\\ \mathbf{Q}\end{Bmatrix} = \begin{bmatrix}-\mathbf{A}^{\mathrm{T}} & \mathbf{B}\\ \mathbf{C} & \mathbf{A}\end{bmatrix}\begin{Bmatrix}\mathbf{P}\\ \mathbf{Q}\end{Bmatrix} - \begin{Bmatrix}\mathbf{F}\\ \mathbf{0}\end{Bmatrix} \tag{8}$$

in which

$$-\mathbf{A}^{\mathrm{T}} = \mathbf{G}_1^{\mathrm{T}} + \mathbf{G}_2^{\mathrm{T}}\mathbf{\Phi}_{21} = \begin{bmatrix} 0 & 0 & k_8\alpha & k_{10}\alpha \\ 0 & 0 & k_9\beta & k_{11}\beta \\ -\alpha & -\beta & 0 & 0 \\ k_6\alpha & k_7\beta & 0 & 0 \end{bmatrix} \quad \mathbf{A} = -(\mathbf{G}_1 + \mathbf{\Phi}_{21}^{\mathrm{T}}\mathbf{G}_2) = \begin{bmatrix} 0 & 0 & -\alpha & k_6\alpha \\ 0 & 0 & -\beta & k_7\beta \\ k_8\alpha & k_9\beta & 0 & 0 \\ k_{10}\alpha & k_{11}\beta & 0 & 0 \end{bmatrix}$$

$$\mathbf{B} = \mathbf{B}^{\mathrm{T}} = \mathbf{G}_2^{\mathrm{T}}\mathbf{\Phi}_{22}\mathbf{G}_2 - \mathbf{\Omega} = \begin{bmatrix} -k_{12}\alpha^2 - k_{15}\beta^2 - \rho\omega^2 & -k_{13}\alpha\beta - k_{15}\beta\alpha & 0 & 0 \\ -k_{13}\alpha\beta - k_{15}\beta\alpha & -k_{14}\beta^2 - k_{15}\alpha^2 - \rho\omega^2 & 0 & 0 \\ 0 & 0 & -\rho\omega^2 & 0 \\ 0 & 0 & 0 & -k_{16}\alpha^2\beta^2 - k_{17}\beta^2 \end{bmatrix}$$

$$\mathbf{C} = \mathbf{C}^{\mathrm{T}} = \mathbf{\Phi}_{11} = \begin{bmatrix} k_1 & 0 & 0 & 0 \\ 0 & k_2 & 0 & 0 \\ 0 & 0 & k_3 & k_4 \\ 0 & 0 & k_4 & k_5 \end{bmatrix}$$

Note, owing to the integration by parts

$$\mathbf{G}_1^{\mathrm{T}} = -\begin{bmatrix} 0 & 0 & 0 & 0 \\ 0 & 0 & 0 & 0 \\ \alpha & \beta & 0 & 0 \\ 0 & 0 & 0 & 0 \end{bmatrix} \quad \mathbf{G}_2^{\mathrm{T}} = -\begin{bmatrix} \alpha & 0 & \beta & 0 & 0 \\ 0 & \beta & \alpha & 0 & 0 \\ 0 & 0 & 0 & 0 & 0 \\ 0 & 0 & 0 & \alpha & \beta \end{bmatrix}$$

Eq. (8) is usually called the state-vector equation. Lee and Jiang (1996) also derived the equation from the field equations for piezoelectricity, but it is not a simple task, especially in some areas such as shells of piezoelectricity. This is one of reasons that we firstly establish the modified mixed variational principle for three-dimensional piezoelectric plates.

Of course, not just the plates or shell have the state space model, if the first-order and high-order beam theories are used, the analytical solutions of the similar state space model for the plate of Fig. 1(b) with SS boundaries can also be obtained with the aid of the state-space approach and Jordan canonical form (Aldraihem and Khdeir, 2003a,b).

Consider a simply supported and multilayered rectangular piezoelectric laminates or hybrid laminates, as shown in Fig. 1(a), the boundary conditions are

$$\begin{aligned} &\text{at } x = 0, a \quad \sigma_x = w = v = \phi = 0 \\ &\text{at } y = 0, b \quad \sigma_y = w = u = \phi = 0 \end{aligned} \tag{9}$$

The state variables, which exactly satisfy the boundary conditions, can be expressed in the following form:

$$\begin{aligned} &\tau_{xz} = \sum_m^\infty \sum_n^\infty \sigma_{xz}^{mn}(z)\cos(\eta x)\sin(\zeta y) \quad \tau_{yz} = \sum_m^\infty \sum_n^\infty \sigma_{yz}^{mn}(z)\sin(\eta x)\cos(\zeta y) \\ &\tau_z = \sum_m^\infty \sum_n^\infty \sigma_z^{mn}(z)\sin(\eta x)\sin(\zeta y) \quad D_z = \sum_m^\infty \sum_n^\infty D_z^{mn}(z)\sin(\eta x)\sin(\zeta y) \\ &u = \sum_m^\infty \sum_n^\infty u^{mn}(z)\cos(\eta x)\sin(\zeta y) \quad v = \sum_m^\infty \sum_n^\infty v^{mn}(z)\sin(\eta x)\cos(\zeta y) \\ &w = \sum_m^\infty \sum_n^\infty w^{mn}(z)\sin(\eta x)\sin(\zeta y) \quad \phi = \sum_m^\infty \sum_n^\infty \phi^{mn}(z)\sin(\eta x)\sin(\zeta y) \end{aligned} \tag{10}$$

where $\eta = m\Pi/a,\ \zeta = n\Pi/b$.

Substituting Eq. (10) into Eq. (8), a system of ordinary differential equations of arbitrary layer can be expressed in the matrix form

$$\frac{\mathrm{d}}{\mathrm{d}z}\begin{Bmatrix} \mathbf{P}^{mn}(z) \\ \mathbf{Q}^{mn}(z) \end{Bmatrix} = \mathbf{K}\begin{Bmatrix} \mathbf{P}^{mn}(0) \\ \mathbf{Q}^{mn}(0) \end{Bmatrix} + \begin{Bmatrix} \mathbf{F}^{mn}(z) \\ \mathbf{0} \end{Bmatrix} \tag{11}$$

where

$$\mathbf{K} = \begin{bmatrix} 0 & 0 & k_8\eta & k_{10}\eta & k_{12}\eta^2 + k_{15}\zeta^2 - \rho\omega^2 & k_{13}\eta\zeta + k_{15}\eta\zeta & 0 & 0 \\ 0 & 0 & k_9\zeta & k_{11}\zeta & k_{13}\eta\zeta + k_{15}\eta\zeta & k_{14}\zeta^2 + k_{15}\eta^2 - \rho\omega^2 & 0 & 0 \\ \eta & \zeta & 0 & 0 & 0 & 0 & -\rho\omega^2 & 0 \\ -k_6\eta & -k_7\zeta & 0 & 0 & 0 & 0 & 0 & k_{16}\eta^2 + k_{17}\zeta^2 \\ k_1 & 0 & 0 & 0 & 0 & 0 & -\eta & k_6\eta \\ 0 & k_2 & 0 & 0 & 0 & 0 & -\zeta & k_7\zeta \\ 0 & 0 & k_3 & k_4 & -k_8\eta & -k_9\zeta & 0 & 0 \\ 0 & 0 & k_4 & k_5 & -k_{10}\eta & -k_{11}\zeta & 0 & 0 \end{bmatrix}$$

The exact solution to Eq. (11) for kth layer is

$$\mathbf{R}_k(z) = \mathbf{T}_k(z)\mathbf{R}_k(0) + \mathbf{H}_k(z) \tag{12}$$

in which

$$\mathbf{R}_k(z) = [\,\mathbf{P}^{mn}(z) \quad \mathbf{Q}^{mn}(z)\,]^{\mathrm{T}} \quad \mathbf{R}_k(0) = [\,\mathbf{P}^{mn}(0) \quad \mathbf{Q}^{mn}(0)\,]^{\mathrm{T}}$$

$$\mathbf{T}_k(z) = \exp(\mathbf{K}\cdot z) \quad \mathbf{H}_k(z) = \int_0^z \exp(\mathbf{K}(z-\tau))\mathbf{F}^{mn}(\tau)\,\mathrm{d}\tau$$

For static problem, if σ_z, D_z and ϕ applied on the surface of the plate are known complex function about x and y, we can expand σ_z, D_z and ϕ into infinite double Fourier series and then adding the response together term by term.

$$\begin{Bmatrix} \sigma_z^{mn} \\ D_z^{mn} \\ \phi^{mn} \end{Bmatrix} = \frac{4}{ab}\int_0^a \int_0^b \begin{Bmatrix} \sigma_z \\ D_z \\ \phi \end{Bmatrix} \sin(\eta x)\sin(\zeta y)\,\mathrm{d}x\,\mathrm{d}y$$

in which

σ_z^{mn}, D_z^{mn} and ϕ^{mn} are the coefficients of the Fourier series.
a and b are the width and length of plate, respectively.

For free vibration, the boundary conditions on the top and bottom surfaces are traction free, which can be state as

$$\sigma_z = \tau_{xz} = \tau_{yz} = 0$$

In addition to the mechanical boundary condition, the electric surface conditions must be satisfied. When the direct piezoelectric effect is considered, the surface of piezoelectric layer is charged free, $D_z = 0$. While the inverse piezoelectric effect is considered, the top and bottom surfaces of the piezoelectric layer are grounded, $\phi = 0$. These two cases are termed open and closed circuit, respectively.

2.3. Elemental state-vector equation

The structure is considered as an n-layered plate.

The field functions and the shape functions of a linear quadrilateral element, which has four-nodes and eight-degree of freedom per node, are assumed as follows (Fig. 2 shows the local coordinate system of the quadrilateral element)

$$\begin{aligned} &u = [\mathbf{N}(x,y)]\{\mathbf{u}^e(z)\} \quad v = [\mathbf{N}(x,y)]\{\mathbf{v}^e(z)\} \quad w = [\mathbf{N}(x,y)]\{\mathbf{w}^e(z)\} \\ &\phi = [\mathbf{N}(x,y)]\{\boldsymbol{\phi}^e(z)\} \quad \tau_{xz} = [\mathbf{N}(x,y)]\{\boldsymbol{\tau}_{xz}^e(z)\} \quad \tau_{yz} = [\mathbf{N}(x,y)]\{\boldsymbol{\tau}_{yz}^e(z)\} \\ &\sigma_z = [\mathbf{N}(x,y)]\{\boldsymbol{\sigma}_z^e(z)\} \quad D_z = [\mathbf{N}(x,y)]\{\mathbf{D}_z^e(z)\} \end{aligned} \tag{13}$$

$$\mathbf{N}_i(\xi,\eta) = \frac{1}{4}(1+\xi_i\xi)(1+\eta_i\eta) \quad i = 1,2,3,4 \tag{14}$$

The discretization is employed in the x–y plane of a layer, as shown in Fig. 3(a).

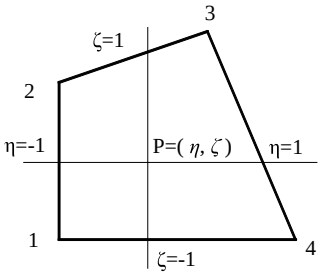

Fig. 2. The local coordinate system of the linear quadrilateral element.

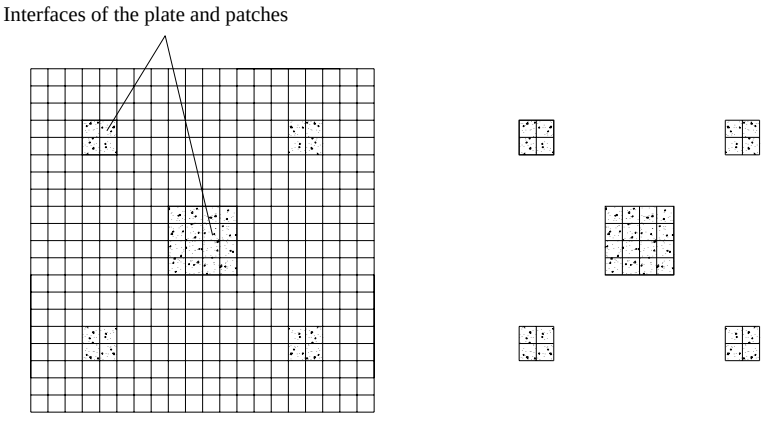

(a) The element meshes of plate (b) The element meshes of patches

Fig. 3. The element mesh of the plate and patches: (a) the element meshes of plate and (b) the element meshes of patches.

Substituting Eqs. (13) and (14) into Eq. (4) and using $\delta\prod = 0$ yields elemental state-vector equation

$$\mathbf{C}^e \frac{\partial \mathbf{R}^e(z)}{\partial z} = \mathbf{K}^e \mathbf{R}^e(z) + \mathbf{G}^e(z) \tag{15}$$

The detailed forms of $\mathbf{C}^e, \mathbf{K}^e, \mathbf{R}^e(z)$, and $\mathbf{G}^e(z)$ can be found in Appendix A.

The treatments on the various boundary conditions are similar to the approaches used in reference (Sheng and Ye, 2002).

The standard finite element assemblage process is employed. Hence the global state-vector equation for kth layer can be obtained

$$\mathbf{C}_k \frac{\partial \mathbf{R}_k(z)}{\partial z} = \mathbf{K}_k \mathbf{R}_k(z) + \mathbf{G}_k(z) \tag{16}$$

The exact solution to Eq. (16) is

$$\mathbf{R}_k(z) = \mathbf{T}_k(z)\mathbf{R}(0) + \mathbf{H}_k(z) \tag{17}$$

in which

$$\mathbf{T}_k = \exp(\mathbf{C}_k\mathbf{K}_k \cdot z) \quad \mathbf{H}_k(z) = \int_0^z \exp(\mathbf{C}_k\mathbf{K}_k(z-\tau))\mathbf{C}_k\mathbf{G}_k(\tau)\,\mathrm{d}\tau$$

Note that, the exponential matrix $\mathbf{T}(z) = \exp(\mathbf{A} \cdot z)$ could be computed in many ways such as approximation theory, differential equations, the matrix eigenvalues, and the matrix characteristics polynomial and so on. In practice, the consideration of computational stability, efficiency and accuracy indicates that some of the methods are preferable to others, but none is completely satisfactory (Moler and Van, 1978). Hence, the precise integration method (Zhong and Zhu, 1996; Zhong, 2001) is employed to solve Eq. (16).

In fact, Eq. (17) or Eq. (12) is available to every layer of laminates. In particular, for the case of $z = h_j$

$$\mathbf{R}_j(h_j) = \mathbf{T}_j(h_j)\mathbf{R}_j(0) + \mathbf{H}_j(h_j) \tag{18}$$

At the interface, the compatibility conditions can be written as

$$\mathbf{R}_j(h_j) = \mathbf{R}_{j+1}(h_j) \quad (j = 1, 2, \ldots, n-1) \tag{19}$$

Hence, the following recurrence formulation can be obtained:

$$\mathbf{R}_n(h_n) = \left(\prod_{i=1}^{n}\mathbf{T}_i\right)\mathbf{R}_1(0) + \left(\prod_{i=2}^{n}\mathbf{T}_i\right)\mathbf{H}_1(h_1) + \left(\prod_{i=3}^{n}\mathbf{T}_i\right)\mathbf{H}_2(h_2) + \cdots + \mathbf{H}_n(h_n) \tag{20}$$

Eq. (20) can be recast into a matrix form

$$\begin{Bmatrix}\mathbf{P}_n(h_n^{\mathrm{p}})\\ \mathbf{Q}_n(h_n^{\mathrm{p}})\end{Bmatrix} = \begin{bmatrix}\mathbf{T}_{11}^{\mathrm{p}} & \mathbf{T}_{12}^{\mathrm{p}}\\ \mathbf{T}_{21}^{\mathrm{p}} & \mathbf{T}_{22}^{\mathrm{p}}\end{bmatrix}\begin{Bmatrix}\mathbf{P}_1(0)\\ \mathbf{Q}_1(0)\end{Bmatrix} + \begin{Bmatrix}\mathbf{H}_{\sigma}^{\mathrm{p}}\\ \mathbf{H}_{u}^{\mathrm{p}}\end{Bmatrix} \tag{21a}$$

where superscript 'p' denotes the laminated plate; $\mathbf{P}_1(0)$, $\mathbf{Q}_1(0)$, $\mathbf{P}_n(h_n)$, $\mathbf{Q}_n(h_n)$ denote the generalized stress vector and displacement vector at the top and bottom surfaces, respectively; $\mathbf{H}_{\sigma}^{\mathrm{p}}$ and $\mathbf{H}_{u}^{\mathrm{p}}$ denote the equivalent external load.

Eq. (21a) is the relationship of the physics quantities of top and bottom surface of an n-layered plate.

The patches are also considered as an l-layered plate, and assuming the element mesh in every layer is the same as the shaded part of Fig. 3(a). The similar procedure above for the top and bottom patches is performed, and yields following equations

$$\begin{Bmatrix}\mathbf{P}_l(h_l^{\mathrm{tp}})\\ \mathbf{Q}_l(h_l^{\mathrm{tp}})\end{Bmatrix} = \begin{bmatrix}\mathbf{T}_{11}^{\mathrm{tp}} & \mathbf{T}_{12}^{\mathrm{tp}}\\ \mathbf{T}_{21}^{\mathrm{tp}} & \mathbf{T}_{22}^{\mathrm{tp}}\end{bmatrix}\begin{Bmatrix}\mathbf{P}_1(0^{\mathrm{tp}})\\ \mathbf{Q}_1(0^{\mathrm{tp}})\end{Bmatrix} + \begin{Bmatrix}\mathbf{H}_{\sigma}^{\mathrm{tp}}\\ \mathbf{H}_{u}^{\mathrm{tp}}\end{Bmatrix} \tag{21b}$$

$$\begin{Bmatrix}\mathbf{P}_l(h_l^{\mathrm{bp}})\\ \mathbf{Q}_l(h_l^{\mathrm{bp}})\end{Bmatrix} = \begin{bmatrix}\mathbf{T}_{11}^{\mathrm{bp}} & \mathbf{T}_{12}^{\mathrm{bp}}\\ \mathbf{T}_{21}^{\mathrm{bp}} & \mathbf{T}_{22}^{\mathrm{bp}}\end{bmatrix}\begin{Bmatrix}\mathbf{P}_1(0^{\mathrm{bp}})\\ \mathbf{Q}_1(0^{\mathrm{bp}})\end{Bmatrix} + \begin{Bmatrix}\mathbf{H}_{\sigma}^{\mathrm{bp}}\\ \mathbf{H}_{u}^{\mathrm{bp}}\end{Bmatrix} \tag{21c}$$

where superscript 'tp' and 'bp' denote the top and the bottom patches, respectively.

The generalized displacements and stresses on the interface between plate and piezoelectric patches must be continuous. Uniting Eqs. (21a)–(21c) yields

$$\begin{Bmatrix}\mathbf{P}(z)\\ \mathbf{Q}(z)\end{Bmatrix} = \begin{bmatrix}\mathbf{T}_{11} & \mathbf{T}_{12}\\ \mathbf{T}_{21} & \mathbf{T}_{22}\end{bmatrix}\begin{Bmatrix}\mathbf{P}(0)\\ \mathbf{Q}(0)\end{Bmatrix} + \begin{Bmatrix}\mathbf{H}_{\sigma}\\ \mathbf{H}_{u}\end{Bmatrix} \tag{22}$$

For free vibration problems, the top surface and bottom surface are traction free. Hence, for open circuit case, $\mathbf{P}(0) = \mathbf{P}(z) = \mathbf{0}$ and $\mathbf{H}_{\sigma} = \mathbf{H}_{u} = \mathbf{0}$, the following equation can be derived from Eq. (22)

$$[\mathbf{T}_{12}]\{\mathbf{Q}_1(0)\} = \mathbf{0} \tag{23a}$$

For closed circuit case $\phi = 0$, $D_z \neq 0$, we exchange the locations of variables ϕ_i and D_{zj} (i, j ∈ k, i, j are node number, and k is the total number of node), a new system of equations can be obtained

$$\begin{Bmatrix}\mathbf{P}'(z)\\ \mathbf{Q}'(z)\end{Bmatrix} = \begin{bmatrix}\mathbf{T}'_{11} & \mathbf{T}'_{12}\\ \mathbf{T}'_{21} & \mathbf{T}'_{22}\end{bmatrix}\begin{Bmatrix}\mathbf{P}'(0)\\ \mathbf{Q}'(0)\end{Bmatrix} + \begin{Bmatrix}\mathbf{H}'_{\sigma}\\ \mathbf{H}'_{u}\end{Bmatrix} \tag{24}$$

Because of $\mathbf{P}'(0) = \mathbf{P}'(z) = \mathbf{0}$ and $\mathbf{H}'_{\sigma} = \mathbf{H}'_{u} = \mathbf{0}$, we have

$$[\mathbf{T}'_{12}]\{\mathbf{Q}'(0)\} = \mathbf{0} \tag{23b}$$

To obtain the nontrivial solution of Eq. (23), the determinant of matrix $\mathbf{T}_{12}$ or $\mathbf{T}'_{12}$ must be zero, namely

$$|\,\mathbf{T}_{12}\,| = \mathbf{0} \text{ or } |\,\mathbf{T}'_{12}\,| = \mathbf{0} \tag{25}$$

The nature frequencies can be obtained from Eq. (25) through the use of bisection method (Johnston, 1982).

As far as the static problems are concerned, $\Omega = 0$. Substituting the known values at the top and bottom surface, the ultimate equation can be obtained

$$\{\mathbf{Q}(z)\} = [\mathbf{T}_{21}]\{\mathbf{P}(0)\} + [\mathbf{T}_{22}]\{\mathbf{Q}(0)\} + \{\mathbf{H}_u\} \text{ (for open circuit case)} \tag{26}$$

$$\{\mathbf{Q}'(z)\} = [\mathbf{T}'_{21}]\{\mathbf{P}'(0)\} + [\mathbf{T}'_{22}]\{\mathbf{Q}'(0)\} + \{\mathbf{H}'_u\} \text{ (for closed circuit case)} \tag{27}$$

In-plane quantities $\mathbf{P}_2 = [\sigma_x\ \sigma_y\ \tau_{xy}\ D_x\ D_y]^{\mathrm{T}}$ can be evaluated by the following expression

$$\mathbf{P}_2 = \mathbf{\Phi}_{21}\mathbf{P} + \mathbf{\Phi}_{22}\mathbf{G}_2\mathbf{Q} \tag{28}$$

3. Numerical validation and discussions

3.1. Example 1

Consider a rectangular simply supported piezoelectric laminate composed of PZT-4 on the top and PVDF on the bottom. Both layers have the thickness $h = 0.0025$ m with $a = 2b$. The aspect ratio of $a/H = 10$ is studied. An applied distributed potential $\phi = 10$ V/m^2 on the top surface with both top and bottom surfaces traction free and $D_z = 0$ (open-circuit case).

The material properties are listed in the following Table 1.

Table 2 shows when the total of elements of both the linear quadrilateral element and the brick element SOLID5 in ANSYS®, which has eight-nodes and four-degree of freedom per node, is equal, the total of degree of frees using present linear quadrilateral element is less than that using the brick element SOLID5.

Fig. 4 shows the convergence rate of the linear quadrilateral element and the brick element SOLID5. When the total elements of present method and ANSYS method are the same (648), the presented solution is $w_{\max} = 1.0531\text{E}{-10}$ (m) and the absolute error is 1.444%; but the solution of ANSYS is $w_{\max} = 0.9927\text{E}{-10}$ (m) and the absolute error is 7.094%. When the total elements of ANSYS method

Table 1
Elastic, piezoelectric, and dielectric properties of piezoelectric materials

Property	C'_{11}	C'_{22}	C'_{33}	C'_{12}	C'_{13}	C'_{23}	C'_{44}	C'_{55}	C'_{66}
PVDF (GPa)	238.00	23.60	10.6	3.98	2.19	1.92	2.15	4.40	6.43
PZT-4 (GPa)	139.00	139.00	115.00	77.80	74.30	74.30	25.60	25.60	30.60
PZT-5H (GPa)	126.00	126.00	118.00	79.50	84.10	84.10	23.30	23.00	23.00
	e'_{31}	e'_{32}	e'_{33}	e'_{24}	e'_{15}				
PVDF (C/m^2)	−0.13	−0.14	−0.28	−0.01	−0.01	–	–	–	–
PZT-4 (C/m^2)	−5.20	−5.20	15.08	12.72	12.72	–	–	–	–
PZT-5H (C/m^2)	−6.50	−6.50	23.3	17	17	–	–	–	–
	$\varepsilon'_{11}/\varepsilon'_0$	$\varepsilon'_{22}/\varepsilon'_0$	$\varepsilon'_{33}/\varepsilon'_0$						
PVDF	12.50	11.98	11.98	–	–	–	–	–	–
PZT-4	1475	1475	1300	–	–	–	–	–	–
PZT-5H	1697.5	1697.5	1468.3	–	–	–	–	–	–
	Density								
PVDF (kg/m^3)	–	–	–	–	–	–	–	–	–
PZT-4 (kg/m^3)	–	–	–	–	–	–	–	–	–
PZT-5H (kg/m^3)	7500	–	–	–	–	–	–	–	–

Note: $\varepsilon'_0 = 8.854 \times 10^{-12}$ F/m.

Table 2
The max values w_{max} at the top surface ($m = n = 1$)

Approaches	Meshes, layers	Total elements	Total d.o.fs	w_{max} (m)	Absolute error (%)
Exact solution	–	–	8	1.0685e−10	
Semi-analytical solution	36 × 18, 2	648	5624	1.0531e−10	1.444
ANSYS, element: SOLID5	36 × 18, 2	648	8436	0.9927e−10	7.094
	56 × 28, 6	1568	46284	1.0214e−10	4.408

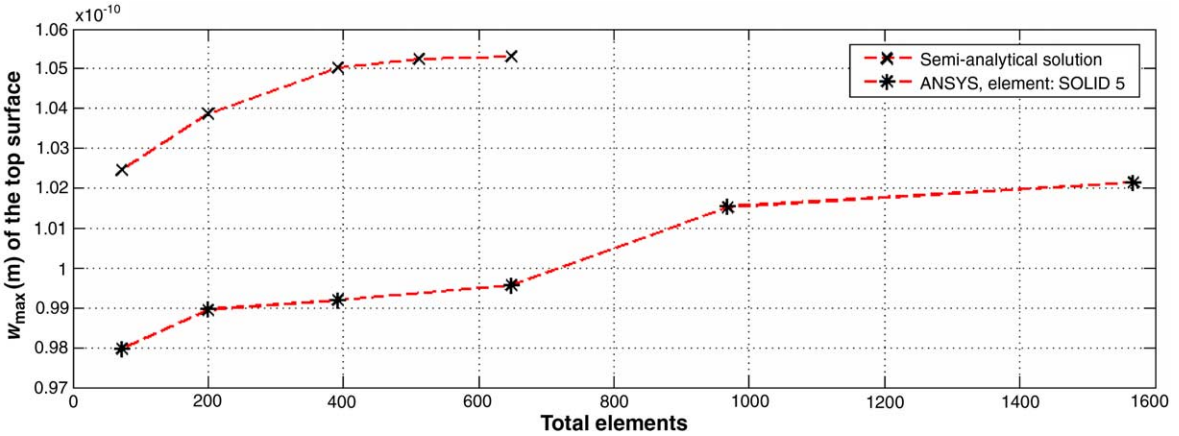

Fig. 4. The comparison of convergence rate.

is 46284, $w_{max} = 1.0214E{-}10$ (m), the absolute error is 4.408%. Hence, it is obvious that the convergence rate of present semi-analytical solution is faster than that of ANSYS. The same conclusion was point out by Sheng and Ye (2002) who employed the similar linear quadrilateral element and used semi-analytical solution to analyze the static problem of laminated composite plates.

3.2. Example 2

The natural frequencies of an aluminum clamped plate with piezoelectric sensors and actuators, as shown in Fig. 1(b), is investigated. Assuming the sensors and actuators are bonded perfectly to the plate. Sensors and actuators made of PZT-5H. The properties of PZT-5H are listed in Table 1. The polarity of both sensors and actuator are in the positive transverse direction (z). The material of plate is aluminum, modulus = 6.8E+10 N/m^2, Poisson's ratio = 0.32, density = 2800 kg/m^3.

It can be noticed in Table 3 that, we use the same linear quadrilateral element and the same mesh density (Lim et al., 2002) to discretize plate and piezoelectric patches, the natural frequencies are higher than those

Table 3
Comparison of natural frequencies (Hz) for a clamped smart plate with piezoelectric patches at the top and bottom surfaces

Approaches Lim et al. (2002)	Meshes, layers			Mode number (open circuit case)						
	Plate	Big patches	Small patches	1	2	3	4	5	6	7
Present	12 × 12, 1	2 × 2, 1	1 × 1, 1	70.4	150.5	220.2	254.4	290.6	334.8	–
	12 × 12, 1	2 × 2, 1	1 × 1, 1	71.6	152.2	223.7	259.1	297.7	343.6	454.7
	20 × 20, 1	4 × 4, 1	2 × 2, 1	69.6	148.2	217.8	251.6	286.7	328.5	442.2

obtained by Lim et al. (2002). In reference (Lim et al., 2002), most part of plate was modeled by 9-node shell elements, the transition portions were modeled by 13-node transition element, the parts of plate between sensor and actuator were modeled by 20-node brick element. It is well-known that the 20-node brick element, the 13-node hexahedron element and the 9-node flat-shell element lead to less unnatural stiffening of the structure and yield better results than do the 8-node brick element, the 6-node hexahedron and the 4-node flat-shell element.

The results in Table 3 also indicate that, as the mesh density increases, the present method yields more accurate results.

4. Conclusions

In this paper, a realistic mathematical model for the static and dynamic analysis of a plate with piezoelectric patches is introduced. In this model, the plate and the piezoelectric patches are discretized by the same linear quadrilateral element. The linear algebraic equations of the plate and piezoelectric patches are established independently. The compatibility of generalized displacements and generalized stresses at the interface between the plate and patches are maintained through uniting the algebraic equation of both of them. The results of the numerical examples show that the current approach offers good predictive capability. Based upon the mathematical model studied in this paper, the following remarks can be made:

1. The number of variables included in the global linear equation of the structures has no relationship with the thickness of plate and the thickness or/and the number of patches.
2. There is no restriction on the thickness of plate or piezoelectric patches.
3. The transverse shear deformation and the rotary inertia are considered in the current model.
4. The semi-analytical solution can also provide continuous generalized stresses and generalized displacements at the interface between plate and piezoelectric patches.

The presented method will be modified to achieve a semi-analytical solution for the transient responses to dynamic loading and the vibration control of the laminated plates with piezoelectric patches or piezoelectric stiffeners.

Acknowledgement

This work was supported by the National Natural Science Foundation of China (Grant No.10072038). The authors would like to express their thanks to reviewers for their valuable comments.

Appendix A

The matrices $\mathbf{G}_1$, $\mathbf{G}_2$, $\mathbf{\Phi}_{11}$, $\mathbf{\Phi}_{12}$, $\mathbf{\Phi}_{21}$, $\mathbf{\Phi}_{22}$ and $\mathbf{\Omega}$ in Eq. (8)

$$\mathbf{G}_1 = \begin{bmatrix} 0 & 0 & \alpha & 0 \\ 0 & 0 & \beta & 0 \\ 0 & 0 & 0 & 0 \\ 0 & 0 & 0 & 0 \end{bmatrix} \quad \mathbf{G}_2 = \begin{bmatrix} \alpha & 0 & 0 & 0 \\ 0 & \beta & 0 & 0 \\ \beta & \alpha & 0 & 0 \\ 0 & 0 & 0 & \alpha \\ 0 & 0 & 0 & \beta \end{bmatrix}$$

$$\mathbf{\Phi}_{12} = -\mathbf{\Phi}_{21}^{\mathrm{T}} = \begin{bmatrix} 0 & 0 & 0 & k_6 & 0 \\ 0 & 0 & 0 & 0 & k_7 \\ k_8 & k_9 & 0 & 0 & 0 \\ k_{10} & k_{11} & 0 & 0 & 0 \end{bmatrix} \quad \mathbf{\Phi}_{22} = \mathbf{\Phi}_{22}^{\mathrm{T}} = \begin{bmatrix} k_{12} & k_{13} & 0 & 0 & 0 \\ k_{13} & k_{14} & 0 & 0 & 0 \\ 0 & 0 & k_{15} & 0 & 0 \\ 0 & 0 & 0 & k_{16} & 0 \\ 0 & 0 & 0 & 0 & k_{17} \end{bmatrix}$$

$$\mathbf{\Phi}_{11} = \begin{bmatrix} k_1 & 0 & 0 & 0 \\ 0 & k_2 & 0 & 0 \\ 0 & 0 & k_3 & k_4 \\ 0 & 0 & k_4 & k_5 \end{bmatrix} \quad \mathbf{\Omega} = \begin{bmatrix} \rho\omega^2 & 0 & 0 & 0 \\ 0 & \rho\omega^2 & 0 & 0 \\ 0 & 0 & \rho\omega^2 & 0 \\ 0 & 0 & 0 & 0 \end{bmatrix}$$

$$k_1 = 1/C'_{55} \quad k_2 = 1/C'_{55} \quad k = C'_{33}\varepsilon'_{33} + e'^2_{33} \quad k_3 = \varepsilon'_{33}/k \quad k_4 = e'_{33}/k$$
$$k_5 = -C'_{33}/k \quad k_6 = -e'_{15}/C'_{55} \quad k_7 = -e'_{24}/C'_{44}$$
$$k_8 = -(C'_{13}\varepsilon'_{33} + e'_{33}e'_{31})/k \quad k_9 = -(C'_{23}\varepsilon'_{33} + e'_{33}e'_{32})/k$$
$$k_{10} = -(C'_{13}e'_{33} - C'_{33}e'_{31})/k \quad k_{11} = -(C'_{23}e'_{33} - C'_{33}e'_{32})/k$$
$$k_{12} = C'_{11} - ((C'_{13}\varepsilon'_{33} + e'_{33}e'_{31})C'_{13} - (C'_{13}e'_{33} - C'_{33}e'_{31})e'_{31})/k$$
$$k_{13} = C'_{12} - ((C'_{13}\varepsilon'_{33} + e'_{33}e'_{31})C'_{23} - (C'_{13}e'_{33} - C'_{33}e'_{31})e'_{32})/k$$
$$k_{14} = C'_{22} - ((C'_{23}\varepsilon'_{33} - e'_{33}e'_{32})C'_{23} - (C'_{23}e'_{33} - C'_{33}e'_{32})e'_{32})/k$$
$$k_{15} = C'_{66} \quad k_{16} = -\varepsilon'_{11} - e'^2_{15}/C'_{55} \quad k_{17} = -\varepsilon'_{22} - e'^2_{24}/C'_{44}$$

Eq. (15) has the following form:

$$\begin{bmatrix} \mathbf{M}^e & \mathbf{0} \\ \mathbf{0} & \mathbf{M}^e \end{bmatrix} \frac{\mathrm{d}}{\mathrm{d}z} \begin{Bmatrix} \mathbf{P}^e(z) \\ \mathbf{Q}^e(z) \end{Bmatrix} = \begin{bmatrix} \mathbf{K}^e_{11} & \mathbf{K}^e_{12} \\ \mathbf{K}^e_{21} & \mathbf{K}^e_{22} \end{bmatrix} \begin{Bmatrix} \mathbf{P}^e(0) \\ \mathbf{Q}^e(0) \end{Bmatrix} + \begin{Bmatrix} \mathbf{F}^e(z) \\ \mathbf{0} \end{Bmatrix}$$

where

$$\mathbf{M}^e = \int\int \mathrm{diag}(\mathbf{N}^{\mathrm{T}}\mathbf{N}) \mid \mathbf{J} \mid \mathrm{d}\xi\,\mathrm{d}\eta \quad \mathbf{J} = \begin{bmatrix} \left[\frac{\partial \mathbf{N}}{\partial \xi}\right]\{\mathbf{x}^e\} & \left[\frac{\partial \mathbf{N}}{\partial \xi}\right]\{\mathbf{y}^e\} \\ \left[\frac{\partial \mathbf{N}}{\partial \eta}\right]\{\mathbf{x}^e\} & \left[\frac{\partial \mathbf{N}}{\partial \eta}\right]\{\mathbf{y}^e\} \end{bmatrix}$$

$$\mathbf{p}^e(z) = [\,\boldsymbol{\tau}^e_{xz}(z) \quad \boldsymbol{\tau}^e_{yz}(z) \quad \boldsymbol{\sigma}^e_z(z) \quad \mathbf{D}^e_z(z)\,]^{\mathrm{T}} \quad \mathbf{Q}^e(z) = [\,\mathbf{u}^e(z) \quad \mathbf{v}^e(z) \quad \mathbf{w}^e(z) \quad \boldsymbol{\phi}^e(z)\,]^{\mathrm{T}}$$

$$\mathbf{K}^e_{11} = \int\int \begin{bmatrix} \mathbf{0} & \mathbf{0} & -k_8\mathbf{N}^{\mathrm{T}}\alpha\mathbf{N} & -k_9\mathbf{N}^{\mathrm{T}}\beta\mathbf{N} \\ \mathbf{0} & \mathbf{0} & -k_{10}\mathbf{N}^{\mathrm{T}}\alpha\mathbf{N} & -k_{11}\mathbf{N}^{\mathrm{T}}\beta\mathbf{N} \\ \mathbf{N}^{\mathrm{T}}\alpha\mathbf{N} & \mathbf{N}^{\mathrm{T}}\beta\mathbf{N} & \mathbf{0} & \mathbf{0} \\ -k_6\mathbf{N}^{\mathrm{T}}\alpha\mathbf{N} & -k_7\mathbf{N}^{\mathrm{T}}\beta\mathbf{N} & \mathbf{0} & \mathbf{0} \end{bmatrix} \mid \mathbf{J} \mid \mathrm{d}\xi\,\mathrm{d}\eta \quad \mathbf{K}^e_{22} = -[\mathbf{K}^e_{11}]^{\mathrm{T}}$$

$$\mathbf{K}^e_{21} = \int\int \begin{bmatrix} k_1\mathbf{N}^{\mathrm{T}}\mathbf{N} & \mathbf{0} & \mathbf{0} & \mathbf{0} \\ \mathbf{0} & k_2\mathbf{N}^{\mathrm{T}}\mathbf{N} & \mathbf{0} & \mathbf{0} \\ \mathbf{0} & \mathbf{0} & k_3\mathbf{N}^{\mathrm{T}}\mathbf{N} & k_4\mathbf{N}^{\mathrm{T}}\mathbf{N} \\ \mathbf{0} & \mathbf{0} & k_4\mathbf{N}^{\mathrm{T}}\mathbf{N} & k_5\mathbf{N}^{\mathrm{T}}\mathbf{N} \end{bmatrix} \mid \mathbf{J} \mid \mathrm{d}\xi\,\mathrm{d}\eta$$

$$\mathbf{K}_{12}^{e}=\int\int\begin{bmatrix}\mathbf{a}-\rho\omega^{2}\mathbf{N}^{\mathrm{T}}\mathbf{N} & \mathbf{b} & \mathbf{0} & \mathbf{0}\\ \mathbf{c} & \mathbf{d}-\rho\omega^{2}\mathbf{N}^{\mathrm{T}}\mathbf{N} & \mathbf{0} & \mathbf{0}\\ \mathbf{0} & \mathbf{0} & -\rho\omega^{2}\mathbf{N}^{\mathrm{T}}\mathbf{N} & \mathbf{0}\\ \mathbf{0} & \mathbf{0} & \mathbf{0} & k_{16}\alpha\mathbf{N}^{\mathrm{T}}\alpha\mathbf{N}+k_{17}\beta\mathbf{N}^{\mathrm{T}}\beta\mathbf{N}\end{bmatrix}\mid\mathbf{J}\mid\mathrm{d}\xi\,\mathrm{d}\eta$$

$$\mathbf{a}=k_{12}\alpha\mathbf{N}^{\mathrm{T}}\alpha\mathbf{N}+k_{15}\beta\mathbf{N}^{\mathrm{T}}\beta\mathbf{N}\quad\mathbf{b}=k_{13}\alpha\mathbf{N}^{\mathrm{T}}\beta\mathbf{N}+k_{15}\beta\mathbf{N}^{\mathrm{T}}\alpha\mathbf{N}$$
$$\mathbf{c}=k_{13}\beta\mathbf{N}^{\mathrm{T}}\alpha\mathbf{N}+k_{15}\alpha\mathbf{N}^{\mathrm{T}}\beta\mathbf{N}\quad\mathbf{d}=k_{14}\beta\mathbf{N}^{\mathrm{T}}\beta\mathbf{N}+k_{15}\alpha\mathbf{N}^{\mathrm{T}}\alpha\mathbf{N}\qquad\begin{Bmatrix}\alpha\\ \beta\end{Bmatrix}=\mathbf{J}^{-1}\begin{Bmatrix}\partial/\partial\xi\\ \partial/\partial\eta\end{Bmatrix}$$
$$\mathbf{F}^{\mathbf{e}}=-\int\int\begin{bmatrix}\mathbf{N}^{\mathrm{T}}f_{x} & \mathbf{N}^{\mathrm{T}}f_{y} & \mathbf{N}^{\mathrm{T}}f_{z} & \mathbf{N}^{\mathrm{T}}f_{q}\end{bmatrix}\mid\mathbf{J}\mid\mathrm{d}\xi\,\mathrm{d}\eta$$

References

Aldraihem, O.J., Khdeir, A.A., 2003a. Exact deflection solutions of beams with shear piezoelectric actuators. International of Solids and Structures 40, 1–12.

Aldraihem, O.J., Khdeir, A.A., 2003b. Precise deflection analysis of beams with piezoelectric patches. Composite Structures 60, 135–143.

Batra, R.C., Liang, X.Q., 1997. The vibration of a rectangular laminated elastic plate with embedded piezoelectric sensors and actuators. Computer and Structure 63, 213–216.

Benjeddou, A., 2000. Advances in piezoelectric finite element modeling of adaptive structural elements: a survey. Computers and Structures 76, 347–363.

Chen, W.Q., Bian, C.F., Ding, H.J., 2004. 3D free vibration analysis of a functionally graded piezoelectric hollow cylinder filled with compressible fluid. International Journal of Solids and Structures 41, 947–964.

Ding, K.W., Tang, L.M., 1999. Three-dimensional free vibration of thick laminated cylindrical shells with clamped edges. Journal of Sound and Vibration 220, 171–177.

Heyliger, P.R., 1994. Static behavior of laminated elastic piezoelectric plates. American Institute of Aeronautics and Astronautics Journal 32, 2481–2484.

Heyliger, P.R., 1997. Exact solutions for simply supported laminated piezoelectric plates. Journal of Applied Mechanics 64, 299–306.

Heyliger, P.R., Brooks, P., 1995. Free vibration of piezoelectric laminates in cylindrical bending. International Journal of Solids and Structures 32, 2945–2959.

Heyliger, P.R., Brooks, P., 1996. Exact solution for laminated piezoelectric plates in cylindrical bending. Journal of Applied Mechanics 63, 903–910.

Heyliger, P.R., Saravanos, D.A., 1995. Exact free vibration analysis of laminated plates with embedded piezoelectric layers. Journal of Acoustic Society of America 98, 1547–1557.

Johnston, R.L., 1982. Numerical Methods. John Wiley, New York.

Kim, J., Kim, J., Varadan, V.V., Varadan, K.V., 1996. Finite-element modeling of a smart cantilever plate and comparison with experiments. Smart Materials and Structures 5, 165–170.

Kim, J., Varadan, V.V., Varadan, K.V., 1997. Finite element modeling of structures including piezoelectric devices. International Journal for Numerical methods in Engineering 40, 817–832.

Lee, J.S., Jiang, L.Z., 1996. Exact electroelastic analysis of piezoelectric laminate via state space approach. International of Solids and Structures 33, 977–990.

Lim, Y., Varadan, V.V., Varadan, K.V., 2002. Closed loop finite-element modeling of active constrained layer damping in the time domain analysis. Smart Materials and Structures 11, 89–97.

Lim, Y., 2003. Finite-element simulation of closed loop vibration control of a smart plate under transient loading. Smart Materials and Structures 12, 272–286.

Moler, C., Van, L.C., 1978. Nineteen dubious ways to compute the exponential of a matrix. SIAM Review (Society for Industrial and Applied Mathematics) 20, 801–836.

Pagano, N.J., 1969. Exact solutions for composite laminates in cylindrical bending. Journal of composites materials 3, 398–411.

Pagano, N.J., 1970. Exact solutions for rectangular bidirectional composites and sandwich plates. Journal of Composite Materials 4, 20–34.

Pagano, N.J., 1972. Dynamic characteristics of composite laminates. Journal of Sound and Vibration 23, 127–143.

Pan, E., 2001. Exact solution for simply supported and multilayered magneto-electro-elastic plates. Journal of Applied Mechanics 68, 608–618.

Pan, E., Heyliger, P.R., 2002. Free vibrations of simply supported and multilayered magneto-electro-elastic plates. Journal of Sound and Vibration 252, 429–442.

Ray, M.C., Rao, K.M., Samanta, B., 1993a. Exact analysis of coupled electroelastic behaviour of a piezoelectric plate under cylindrical bending. Computers and Structures 47, 1031–1042.

Ray, M.C., Bhattacharya, R., Samanta, B., 1993b. Exact analysis for static analysis of intelligent structures. American Institute of Aeronautics and Astronautics Journal 31, 1684–1691.

Ray, M.C., Bhattacharya, R., Samanta, B., 1998. Exact solutions for dynamic analysis of composite plate with distributed piezoelectric layers. Computers and Structures 66, 737–743.

Senthil, S.V., Batra, R.C., 2001. Exact solution for the cylindrical bending of laminated plates with embedded piezoelectric shear actuators. Smart Material Structures 10, 240–251.

Sheng, H.Y., Ye, J.Q., 2002. A state space finite element for laminated composite plates. Computer Methods in Applied Mechanics and Engineering 191, 4259–4276.

Steele, C.R., Kim, Y.Y., 1992. Modified mixed variational principle and the state-vector equation for elastic bodies and shells of revolution. Journal of Applied Mechanics 59, 587–595.

Tarn, J.Q., 2002. A state space formalism for piezothermmoelasticity. International Journal of Solids and structures 39, 5173–5184.

Ting, T.C., 1996. Anisotropic Elasticity. Theory and Application. Oxford University Press, New York.

Vel, S.S., Batra, R.C., 2000. Three-dimensional analytical solution for hybrid multilayered piezoelectric plates. Journal of Applied Mechanics 67, 558–567.

Wang, J.G., Fang, S.S., Chen, L.F., 2002. The state vector methods for space axisymmetric problems in multilayered piezoelectric media. International Journal of Solids and Structures 39, 3959–3970.

Wang, J.G., Chen, L.F., Fang, S.S., 2003. State vector approach to analysis of multilayered magneto-electro-elastic plates. International Journal of Solids and structures 40, 1669–1680.

Zhong, W.X., 1995. A New Systematic Methodology for Theory of Elasticity. Dalian University of Technology Press.

Zhong, W.X., Zhu, J.P., 1996. Precise time integration for the matrix Riccati differential equation. Journal on Numerical Methods in Computer Applications 17, 26–35.

Zhong, W.X., 2001. Combined method for the solution of asymmetrical Riccati differential equations. Computer Methods in Mechanics and Engineering 191, 93–102.

Zou, G.P., Tang, L.M., 1995. A semi-analytical solution for thermal stress analysis of laminated composite plates in the Hamiltonian system. Computers and Structures 55, 113–118.